

PHYSICAL PARAMETERS IN THE HOT SPOTS AND JETS OF COMPACT SYMMETRIC OBJECTS

M. PERUCHO¹ AND J. M. ^AMARTÍ¹

Draft version October 31, 2018

ABSTRACT

We present a model to determine the physical parameters of jets and hot spots of a sample of CSOs under very basic assumptions like synchrotron emission and minimum energy conditions. Based on this model we propose a simple evolutionary scenario for these sources assuming that they evolve in ram pressure equilibrium with the external medium and constant jet power. The parameters of our model are constrained from fits of observational data (radio luminosity, hot spot radius and hot spot advance speed) versus projected linear size. From these plots we conclude that CSOs evolve self-similarly and that their radio luminosity increases with linear size along the first kiloparsec. Assuming that the jets feeding CSOs are relativistic from both kinematical and thermodynamical points of view, we use the values of the pressure and particle number density within the hot spots to estimate the fluxes of momentum (thrust), energy, and particles of these relativistic jets. The mean jet power obtained in this way is within an order of magnitude that inferred for FR II sources, which is consistent with CSOs being the possible precursors of large doubles. The inferred flux of particles corresponds to, for a barionic jet, about a 10% of the mass accreted by a black hole of $10^8 M_{\odot}$ at the Eddington limit, pointing towards a very efficient conversion of accretion flow into ejection, or to a leptonic composition of jets. We have considered three different models (namely Models I, IIa, IIb). Model I assuming constant hot spot advance speed and increasing luminosity can be ruled out on the ground of its energy cost. However Models IIa and IIb seem to describe limiting behaviours of sources evolving at constant advance speed and decreasing luminosity (Model IIa) and decreasing hot spot advance speed and increasing luminosity (Model IIb). In all our models the slopes of the hot spot luminosity and advance speed with source linear size are governed by only one parameter, namely the external density gradient. A short discussion on the validity of models II to describe the complete evolution of powerful radio sources from their CSO phase is also included.

Subject headings: galaxies:active-galaxies;jets-galaxies:ISM-radio continuum:galaxies

1. INTRODUCTION

In the early eighties VLBI techniques allowed the discovery of compact, high luminosity radio sources with double structure and steep spectrum (Phillips & Mutel 1980,1982). Some of them were found to have a core between the two outer components which were interpreted as lobes or hot-spots formed by a relativistic jet, and they were given the name of compact symmetric objects (CSOs) because of their double-sided emission and their small size (linear size lower than 1 kpc).

The spectra of CSOs are steep with a peak at about 1 GHz, what makes them to belong to Gigahertz Peaked Spectrum Sources (GPSs, O’Dea et al. 1991). If the peak is located around 100 Megahertz the source belongs to Compact Steep Spectrum Sources (CSSs, Fanti et al. 1995). The smaller sources are more likely to have a GPS spectrum, while those with a projected linear size larger than one kpc (linear size between 1 and 20 kpc) have a CSS spectrum. GPS and CSS sources include a variety of objects (O’Dea 1998), morphologically speaking, among which we find the double, symmetric ones: CSOs if their size is lower than 1 kpc (Wilkinson et al. 1994), and Medium Size Symmetric Objects, MSOs, if their size does exceed 1 kpc (Fanti et al. 1995). For a review about GPS and CSS sources see O’Dea (1998).

The size of CSOs led radio astronomers to propose two opposed conjectures. One of them assumes a scenario where the external medium is so dense that the jet cannot break its way through it, so sources are old and confined (van Breugel et al. 1984), while the other one assumes that they are the young

precursors of large symmetric sources like Faranoff-Riley type II galaxies (Phillips & Mutel 1982, Carvalho 1985, Mutel & Phillips 1988). The former assumption is based on observations which show that some GPS sources are considerably optically reddened (O’Dea 1991), have distorted isophotes and disturbed optical morphologies, which indicate interaction with other galaxies or mergers. This can be interpreted as that the source has an abnormally dense medium, due to the gas falling onto the nucleus of the GPS from the companion. Under this assumption, sources can be confined by the external medium if it is dense enough (average number density of $10-100 \text{ cm}^{-3}$), as it was shown by De Young (1991,93) through simulations of jet collisions with a dense, cloudy medium. Carvalho (1994,98) considers two scenarios, one where the NLR and ISM consist of a two-phase medium formed by a hot, tenuous one surrounding cold, dense clouds, with which the jet collides, mass loads and slows down, and another one where a uniform, dense external medium is assumed. This could result in the jet having to spend its life trapped within this medium and having ages of 10^6 to 10^7 years. On the other hand, it must be said that densities required for the jet to be confined imply huge masses for the innermost parsecs of the galaxy (De Young 1993).

Recent measurements of component advance speeds for a few sources (Owsianik et al. 1998, Taylor et al. 2000), reveal that their speeds are better understood within the young source model, as they imply ages of no more than 10^3 years. Theoretical evolutionary models have been proposed by Carvalho (1985), Readhead et al. (1996b), Fanti et al. (1995), Begel-

¹Departamento de Astronomía y Astrofísica, Universidad de Valencia, 46100 Burjassot (Valencia), Spain. e-mail: manuel.perucho@uv.es, jose-maria.marti@uv.es

man (1996), O’Dea & Baum (1997), Snellen et al. (2000), in which an attempt is made to establish a connection between CSOs, MSOs, and FR II. Simulations carried out by De Young (1993,97) also show that a jet evolving in a density gradient of a not very dense medium reproduces well those evolutionary steps.

The study of CSOs is of interest because it will allow us to probe conditions in the jet in the first kiloparsec of its evolution and the interaction with the dense interstellar medium before it breaks through the intergalactic medium, where jets have been extensively studied. Jets in CSOs are propagating through the NLR and ISM of AGNs, so this interaction is a good opportunity to get information about the central regions of AGNs, in particular about the central density and its gradient. Moreover, within the young source scenario, jets from CSOs are in the earliest stages after their formation, allowing us to get information and constrain the conditions leading to the jet formation.

In this paper, we obtain the basic physical parameters of jets and hot-spots of a sample of CSOs using very basic assumptions, in a similar way as Readhead et al. (1996a,b), i.e., synchrotron radiation theory, minimum energy assumption and ram pressure equilibrium with the external medium. We also propose a simple evolutionary scenario for them, based on observational data, through a theoretical model which gives the relevant magnitudes in the hot-spots as power laws of linear size. The model allows us to get some insight about the nature of CSOs and their environment, with the final aim of knowing whether these sources are related to large double radio sources. The criteria followed to obtain a sample of CSO and their data are explained in section 2. In section 3, the theory used to get physical parameters for hot-spots out of their spectra is presented. In section 4 we use some basic assumptions to get information about the physical parameters of the jet. Section 5 contains the evolutionary model proposed and comparison with previous models, and conclusions along with further comparisons are presented in section 6. Finally, the relevant formulae used in the calculations of the physical magnitudes of hot-spots are presented in the Appendix. Throughout the paper we consider Hubble constant $H_0 = 100 h \text{ km s}^{-1} \text{ Mpc}^{-1}$, with normalised value $h = 0.7$, and flat universe through a deceleration parameter $q_0 = 0.5$.

2. A SAMPLE OF CSOS

Sources have been selected from the GPS samples of Stanghellini et al. (1997), Snellen et al. (1998, 2000) and Peck & Taylor (2000). We have chosen those sources with double morphology already classified in the literature as CSOs and also those whose components can be safely interpreted as hot spots even though the central core has not been yet identified. The criteria we have followed are quite similar to those used by Peck & Taylor (2000), i.e., detected core surrounded by double radio structure or double structure with edge brightening of both components; however, contrary to their criteria, we have included sources with an intensity ratio between both components greater than 10 in the frequency considered (see Table 1), relaxing this constraint to a value of 20 (in one source, 2128+048) and 11 for the rest. Anyway, sources possibly affected by orientation effects (beaming, spectra distortion) in a more evident way, like quasars and core-jet sources, have not been considered. The resulting sample is formed by 20 sources which are listed in Table 1 along with the data relevant for our study.

3. PHYSICAL PARAMETERS IN THE HOT SPOTS OF CSOS

Panels a) and b) of Fig. 1 display hot spot radius (r_{hs}) and hot spot luminosity (L_{hs}), respectively, versus projected source linear size (LS). These quantities are directly obtained from the corresponding measured (or modeled) angular sizes, flux densities in the optically thin part of the spectra and the formulae for cosmological distance (see Appendix for details). For those hot-spots with more than one component the radius was obtained as the one of the resulting total volume by adding the volumes of each component. One point per source is used by taking arithmetic mean values for the radius and radio-luminosity.

Table 2 compiles the slopes for the corresponding linear log-log fits, the errors and the regression coefficients. A proportionality between hot spot radius and linear size is clearly observed. The hot spot luminosity seems to be independent of the source linear size, with only a weak tendency to grow with LS .

In order to estimate internal physical parameters as the densities and energies of the ultrarelativistic particles in the hot spots, further assumptions should be made. According to the present understanding (see, for example, O’Dea 1998), the peak and inversion in the spectra of these sources is due to an absorption process which has been a matter of debate since the discovery of these objects. First, and most likely, synchrotron self absorption (SSA) may be the reason of the inversion, although Bicknell et al. (1997) and Kuncic et al. (1997), have proposed free-free absorption (FFA) and induced Compton scattering (ICS), respectively, as alternatives. Both latter models are successful in reproducing the decrease in peak frequency with linear size observed in GPS sources (O’Dea & Baum 1997), but do not fit the data better than the SSA model. Also, Snellen et al. (2000) find evidence of SSA being the process of absorption producing the peak in GPS sources. Besides that, FFA and ICS do not allow us to extract information about the hot spot parameters, as absorption occurs in the surrounding medium of the hot-spots, by thermal electrons, whereas SSA occurs inside them.

The problem with SSA model comes from its critical dependence on some parameters (as an example, the magnetic energy density is proportional to the tenth power of the peak frequency and the eighth power of the source angular size) which makes it almost useless for our purposes. Having this in mind, we have relied on the minimum energy assumption, which states that the magnetic field and particle energy distributions arrange in the most efficient way to produce the estimated synchrotron luminosity, as a conservative and consistent way to obtain information about the physical conditions in hot spots. As it is well known, the hypothesis of minimum energy leads almost to equipartition, in which the energy of the particles is equal to that of the magnetic field. Güijosa & Daly (1996) compared equipartition Doppler factors with those obtained assuming that X-ray emission comes from inverse Compton process for more than a hundred objects (including three radio galaxies also in our sample) concluding that they are actually near equipartition. Snellen et al. (2000) point out that sources must stay in equipartition if they are to grow self-similarly, as it seems to be the case (see Table 2. Finally, Table 3 in O’Dea (1998) compiles data from Mutel et al. (1985) and Readhead et al. (1996a), and compares magnetic field estimates in the hot spots of several CSOs based on both minimum energy and SSA models. As both results are in rough agreement, the conclusion is that sources undergo synchrotron self-absorption but are near equipartition. Besides the minimum energy assumption, we also assume that there is no thermal (barionic nor leptonic)

component, so the number density of relativistic particles alone within the hot spots is estimated, and that each particle radiates its energy at the critical frequency, i.e., *monochromaticity*.

The calculation procedure for pressure (P_{hs}) and number density of relativistic particles (n_{hs}) is explained in the Appendix, and panels c) and d) of Fig. 1 represent their log-log plots versus projected source linear size for all the sources in our sample, along with the best linear fit, assuming they all fulfill the minimum energy assumption. As in the case of panels a) and b) one point per source is plotted. We use volume weighted means of both magnitudes due to their intensive character. Slopes, errors, and regression coefficients of the corresponding fits are listed in Table 2.

These plots and their fits may be interpreted as evolutionary tracks of the four magnitudes in terms of the distance to the origin, considering that this distance grows monotonically with time, as we will show in Sect. (5). Projection effects are surely a source of dispersion in the data, which on the other hand show good correlation. One way to test the influence of these projection effects is to use hot-spot radius, as it is not affected by projection, instead of linear size. Results for the fits are very similar (within error bars) to those in Table 2, so it can be stated that projection effects are not important as far as an evolutionary interpretation is concerned. We should keep in mind that we have removed from our sample those sources most likely pointing along the line of sight (quasars and core-jet sources).

We can add to our series of data the recent measurements of hot spot advance speeds (see Table 3). Owsianik & Conway (1998) report a mean hot spot advance speed of $0.13h^{-1}c$ in 0710+439 whereas Owsianik et al. (1998b) conclude a speed of $0.10h^{-1}c$ in 0108+388. On the other hand, Taylor et al. (2000) give similar advance speeds for 0108+388 ($0.12h^{-1}c$) and 2352+495 ($0.16h^{-1}c$) while the speed they measure for 0710+439 is twice the one reported by Owsianik & Conway (1998) ($0.26h^{-1}c$). Finally, Owsianik et al. (1998) derive an estimate for the hot spot advance speed of $0.13h^{-1}c$ for 2352+495, based on synchrotron ageing data from Readhead et al. (1996a) and measurements of the source size.

The large difference of estimates in the case of 0710+439 can be attributed to a number of facts. On one hand, Taylor et al.'s (2000) measurements have been performed at a higher frequency which means that they have measured motions of a brighter and more compact working surface, which must be intrinsically faster than the lobe expansion. On the other hand, the velocity may have suffered a recent increase (Owsianik & Conway 1998 data are concluded from five epochs from 1980 to 1993, whereas Taylor et al.'s 2000 measurements are from three epochs from 1994 to 1999) as the authors point out. We should keep in mind that the jet is moving in a cloudy medium, the NLR or ISM, so measures of advance speed are conditioned by local environmental conditions.

Finally, Taylor et al. (2000) detect motions for 1031+567, also included in our sample, for which an advance speed of $0.31h^{-1}c$ is inferred. However this speed is measured for one hot spot (component W1) and what could be a jet component (component E2) and, therefore, this speed may be overvalued.

The results reported in the previous paragraphs concerning the hot spot advance speeds do not allow us to infer a definite behaviour of the hot spot advance speed with the distance to the source. However, excluding the measurements of Taylor et al. (2000) on 0710+439 and 1031+567 for the above reasons, the remaining results are compatible with a constant expansion

speed ($v_{\text{hs}} \propto LS^0$), that we shall assume as a reference in the evolution models developed in Sect. (5).

4. PHYSICAL PARAMETERS IN THE JETS OF CSOS AND THE SOURCE ENERGY BUDGET

Figure 2 shows a schematic representation of our model for CSOs in which the bright symmetric radio components are hot spots generated by the impact of relativistic jets in the ambient medium. In the following we shall assume that the jets are relativistic from both kinematical and thermodynamical points of view, hence neglecting the effects of any thermal component. We can use the values of the pressure and particle number density within the hot spots to estimate the fluxes of momentum (thrust), energy, and particles of these relativistic jets. Under the previous hypothesis and assuming that hot spots advance at subrelativistic speeds, ram pressure equilibrium between the jet and hot spot leads to (Readhead et al. 1996a)

$$F_j = P_{\text{hs}} A_{\text{hs}}, \quad (1)$$

for the jet thrust F_j , where A_{hs} stands for the hot spot cross section ($\simeq \pi r_{\text{hs}}^2$). Taking mean values for P_{hs} and r_{hs} from our sample we get $F_j \simeq (4.5 \pm 3.3) 10^{34}$ dyn, where errors are calculated as average deviations from the mean.

In a similar way, the flux of relativistic particles in the jet, R_j , can be estimated from the total number of particles in the hot spot, $n_{\text{hs}} V_{\text{hs}}$ (V_{hs} is the hot spot volume, $\simeq 4\pi r_{\text{hs}}^3/3$), and the source lifetime, $\simeq v_{\text{hs}}/LS$, where v_{hs} is the hot spot advance speed. Assuming this speed constant and $\simeq 0.2c$, we can write

$$R_j = n_{\text{hs}} V_{\text{hs}} v_{\text{hs}} / LS \simeq (6.3 \pm 6.2) 10^{48} e^{+/-} s^{-1}. \quad (2)$$

Finally, a lower bound for the jet power, Q_j , can be estimated considering that, in a relativistic jet from a thermodynamic point of view, $Q_j = (F_j/v_j)c^2$. Hence, for given F_j and taking $v_j = c$, we have

$$Q_{j,\text{min}} = F_j c = P_{\text{hs}} A_{\text{hs}} c = (1.3 \pm 1.0) 10^{45} \text{ ergs}^{-1}. \quad (3)$$

Let us point out that the values of the jet power and jet thrust derived according to our model ($4.3 - 5.0 10^{43}$ erg s^{-1} , $1.4 - 1.7 10^{33}$ dyn) are within a factor of 1.5 of those presented by Readhead et al. (1996a) for $h = 0.7$.

Considering that the source spends the jet power in luminosity (basically, hot spot radio luminosity, L_{hs}), advance (Q_{adv}), and expansion of hot spots against the external medium ($Q_{\text{exp,hs}}$), and that a fraction of the energy supplied is stored as internal energy of particles and magnetic fields in the hot spots ($\dot{U}_{\text{int,hs}}$), we can write the following equation for the energy balance

$$Q_j = L_{\text{hs}} + \dot{U}_{\text{int,hs}} + Q_{\text{adv}} + Q_{\text{exp,hs}} + Q_{\text{lobes}}, \quad (4)$$

where the term Q_{lobes} encompasses the energy transferred to the lobes (and cocoon) per unit time. Note that, in the previous equation, we have added the internal energy of the hot spots and the expansion work with respect to the work by Readhead et al. (1996a).

The power invested by the source in advance and expansion of the hot spot and the variation of the internal energy in the hot spot per unit time can be estimated as follows (assuming constant advance speed)

$$\dot{U}_{\text{int,hs}} \approx P_{\text{hs}} V_{\text{hs}} \left(\frac{v_{\text{hs}}}{LS} \right), \quad (5)$$

$$Q_{\text{adv}} \approx P_{\text{hs}} A_{\text{hs}} v_{\text{hs}}, \quad (6)$$

$$Q_{\text{exp,hs}} \approx P_{\text{hs}} 4\pi r_{\text{hs}}^2 v_{\text{hs}} \left(\frac{r_{\text{hs}}}{LS} \right), \quad (7)$$

where in the last expression we have used that the hot spot expansion speed is $v_{\text{exp,hs}} = v_{\text{hs}}(r_{\text{hs}}/LS)$, due to the self-similar evolution of the sources deduced from panel a) of Fig. 1, a result to be discussed in the next section.

Table 4 lists the average powers invested by the source in their evolution for the values of the hot spot parameters derived in the previous section. Despite the large uncertainties it is worthy to note that there seems to be some kind of equipartition between luminosity and expansion (source growth plus hot spot expansion) work per unit time. It has to be noted that percentages are obtained with respect to $Q_{j,\text{min}}$. The remaining fraction, 45%, must be, at least in part, associated with power transferred to the lobes. Finally let us point that the increase of internal energy of the hot spot is a negligible fraction of the jet power.

5. A SELF-SIMILAR EVOLUTION MODEL FOR CSOS

In this section, we are going to construct an evolutionary model for CSOs based on the results presented in section 3. The distance to the origin of the hot-spots will play the role of a time-like coordinate. The fits presented in that section will represent the evolution of the corresponding physical quantity in a typical CSO helping us to constrain the parameters of our model.

Our model is based on the assumption that the evolution of CSOs is dominated by the expansion of the hot spots as they propagate through the external medium. This conclusion is apparent after analysing the source energy budget (see Table 4), as 33% of $Q_{j,\text{min}}$ is invested in expansion.

We start by assuming that the linear size of the hot spot, r_{hs} , grows with some power of time, i.e., $r_{\text{hs}} \propto t^\beta$. We have chosen such a basic parameter because a value of β can be easily deduced from the linear fits, as we shall see below. Our next assumption consists in considering a density decreasing external medium with $\rho_{\text{ext}} \propto (LS)^{-\delta}$, with $\delta > 0$. In order to compare with the observational fits described in the previous section, we need to eliminate t from our description. This is done through the velocity of advance of the hot spot, v_{hs} , that fixes the dependence of the linear size of the source with the time. Considering that hot spots in CSOs are feed by relativistic jets but advance with significantly smaller speeds, the usual ram pressure equilibrium condition between the jet and the external medium leads to (Martí et al. 1997)

$$v_{\text{hs}} = \sqrt{\eta_{\text{R}} \frac{A_{\text{j}}}{A_{\text{j,hs}}}} v_{\text{j}}, \quad (8)$$

where η_{R} is the ratio between the inertial density of the jet and that of the external medium (ρ_{ext}), A_{j} and $A_{\text{j,hs}}$ are, respectively, the cross-sectional area of the jet at the basis and at the hot spot, respectively, and v_{j} is the flow velocity in the jet. We can consider that $A_{\text{j,hs}} \propto r_{\text{hs}}^2$ and this is what we do in the next. Assuming that the jet injection conditions are constant with time we have

$$\left(\frac{dLS}{dt} \right) v_{\text{hs}} \propto \left(\eta_{\text{R}} \frac{A_{\text{j}}}{A_{\text{hs}}} \right)^{1/2} v_{\text{j}} \propto (LS)^{\delta/2} t^{-\beta}, \quad (9)$$

from which we derive the desired relation:

$$t \propto (LS)^{(1-\delta/2)/(1-\beta)}. \quad (10)$$

Evolutionary tracks of sources that grow with time are obtained when the exponent in the later expression is positive, which means that both $\beta, \delta/2 > 1$, or $\beta, \delta/2 < 1$. On the other hand, substituting this latter expression in eq. (9) we find that

$$v_{\text{hs}} = (LS)^{(\delta/2-\beta)/(1-\beta)}, \quad (11)$$

from which we can conclude that the particular case $\beta = \delta/2$ (including the case $\beta = \delta/2 = 1$) leads to a constant hot spot advance speed and separates accelerating hot spot models ($\beta < \min\{1, \delta/2\}$; $\beta > \max\{1, \delta/2\}$) from decelerating ones ($\min\{1, \delta/2\} < \beta < \max\{1, \delta/2\}$).

The hot spot radius in terms of the source linear size follows also from eq. (10)

$$r_{\text{hs}} \propto (LS)^{\beta(1-\delta/2)/(1-\beta)}. \quad (12)$$

Self-similarity forces the exponent in this expression to be equal to 1 providing a relation between β and the slope of the external density profile, δ ,

$$\beta = \frac{2}{4-\delta}, \quad (13)$$

consistent with self-similar source evolution. Deduced from this expression is that $\beta \geq \delta/2$ which means that hot spots tend to decelerate within the first kpc if $\beta < 1$ or to accelerate if $\beta > 1$. We will discuss this result below. Note that our model allows for self-similar evolution tracks with non-constant hot spot advance speeds, contrary to other models (e.g., Begelman 1996).

The next equation in our model comes from the source energy balance. The energy injected by the jet is stored in the hot spots and lobes in the form of relativistic particles, magnetic fields, and thermal material. Besides that, it provides the required energy for the source growth (hot spot expansion and advance, lobe inflation). Finally, it is the ultimate source of luminosity. Being CSO sources immersed in dense environments, a basic assumption is to consider that the work exerted by the hot spots against the external medium consumes a large part of jet power. This is, in fact, supported by the results shown in previous section. Hence we assume

$$(PdV)_{\text{hs,adv+exp}} \propto P_{\text{hs}} r_{\text{hs}}^2 LS \propto t^\gamma, \quad (14)$$

where the intermediate proportionality is, again, only valid for self-similar evolution. A value 1 for γ would mean that the source adjusts its work per unit time to the jet power supply (that we consider as constant).

Finally, under the assumptions of minimum energy and monochromaticity (see Appendix), the luminosity of the hot spot, L_{hs} , and the number density of relativistic particles, n_{hs} , are found to follow the laws

$$L_{\text{hs}} \propto P_{\text{hs}}^{7/4} r_{\text{hs}}^3, \quad (15)$$

$$n_{\text{hs}} \propto P_{\text{hs}}^{5/4}. \quad (16)$$

5.1. Model I (3 parameters)

The equations derived above can be manipulated to provide expressions for v_{hs} , r_{hs} , L_{hs} , P_{hs} , and n_{hs} in terms of source linear size, LS ,

$$v_{\text{hs}} \propto (LS)^{(\delta/2-\beta)/(1-\beta)} \left(\propto (LS)^{\delta/2-1} \right) \quad (17)$$

$$r_{\text{hs}} \propto (LS)^{\beta(1-\delta/2)/(1-\beta)} (\propto LS) \quad (18)$$

$$L_{\text{hs}} \propto (LS)^{(7\gamma/4-\beta/2)(1-\delta/2)/(1-\beta)-7/4} \left(\propto (LS)^{(7\gamma(2-\delta/2)-9)/4} \right) \quad (19)$$

$$P_{\text{hs}} \propto (LS)^{(\gamma-2\beta)(1-\delta/2)/(1-\beta)-1} \left(\propto (LS)^{\gamma(2-\delta/2)-3} \right) \quad (20)$$

$$n_{\text{hs}} \propto (LS)^{5/4((\gamma-2\beta)(1-\delta/2)/(1-\beta)-1)} \left(\propto (LS)^{5/4(\gamma(2-\delta/2)-3)} \right) \quad (21)$$

where we have written in brackets the resulting expressions considering self-similarity, using the relation between β and δ in eq. (13). Now, the first three relations (involving observable quantities) can be compared with the corresponding fits in section (3) to obtain the values of the free parameters in our model, β , γ , and δ . The comparison of the resulting power laws for P_{hs} and n_{hs} with their fits will provide a consistency test of the basic assumptions of our model. For constant hot spot advance speed the results are: $\beta = 1.0 \pm 0.3$, $\delta = 2.0 \pm 0.6$, $\gamma = 1.5 \pm 0.3$, where errors are calculated from the obtained extreme values by changing the slopes of the fits within the given errors. The value of $\beta = 1.0$ corresponds to a constant hot spot expansion speed. The value of $\delta = 2$ is consistent with the external density profile in Begelman's (1996) model, for self-similar, constant growth sources.

The value obtained for γ merits some discussion. In our present model, the increase in luminosity inferred from the fits (and invoked by Snellen et al. 2000 to explain the GPS luminosity function) does not need an external medium with constant density in the first kiloparsec (as concluded by Snellen et al., 2000) but together with constant advance speed require that power invested by the hot spots in the advance and expansion work (see section 4) grows with time as $t^{0.5}$. Taking into account that the expansion against the environment is a substantial fraction of the whole jet power supply, a value of γ larger than 1 implies that the expansion will eventually exhaust the source energy supply, producing a dramatic change in the source evolution (decrease in luminosity, deceleration of the hot spot advance) after the first kiloparsec. Recent calculations, in which we extend our study to MSO and FR II hot spots (Perucho & Martí 2001), show that radio luminosity in the hot spots (as well as the expansion work) decrease in the long term. However, one should keep in mind that the trend of constant hot spot advance speed (and the luminosity growth with linear size) in the CSO phase are largely uncertain.

The corresponding exponents for P_{hs} and n_{hs} (-1.5 ± 0.8 , -1.9 ± 1.0 , respectively) are within the error bars of the fits presented in section 3, giving support to the minimum energy assumption considered in our model.

5.2. Model II (2 parameters)

Model I has three free parameters which were fixed using the observational constraints. However, two of these constraints (namely hot spot luminosity versus source linear size, and hot spot advance speed versus source linear size) are poorly established. This is why we explore in this section two new models with only two free parameters by fixing γ equal to 1. This is a reasonable choice as it expresses that the source self-adjusts the work per unit time to the (assumed constant) power jet supply. On the other hand, fixing one parameter allows us to liberate the models from one constraint allowing for the study of different evolutionary tracks. In particular we are going to study two models, IIa and IIb, although a continuity between them both is also possible, as discussed below.

Making $\gamma = 1$ in eqs. (17)-(21), we have

$$v_{\text{hs}} \propto (LS)^{(\delta/2-\beta)/(1-\beta)} \left(\propto (LS)^{\delta/2-1} \right) \quad (22)$$

$$r_{\text{hs}} \propto (LS)^{\beta(1-\delta/2)/(1-\beta)} (\propto LS) \quad (23)$$

$$L_{\text{hs}} \propto (LS)^{(7/4-\beta/2)(1-\delta/2)/(1-\beta)-7/4} \left(\propto (LS)^{(7(2-\delta/2)-9)/4} \right) \quad (24)$$

$$P_{\text{hs}} \propto (LS)^{(1-2\beta)(1-\delta/2)/(1-\beta)-1} \left(\propto (LS)^{-(\delta/2+1)} \right) \quad (25)$$

$$n_{\text{hs}} \propto (LS)^{5/4((1-2\beta)(1-\delta/2)/(1-\beta)-1)} \left(\propto (LS)^{-5/4(\delta/2+1)} \right) \quad (26)$$

Again results for self-similar evolution appear in brackets. Model IIa uses the fit for the $r_{\text{hs}}-LS$ and constant speed assumption (v_{hs}) to determine the values of β and δ . In Model IIb, the first condition is maintained (self-similarity) whereas the second is changed by the fit for radio-luminosity ($L_{\text{hs}}-LS$). The values of β and δ for Models IIa and IIb as well as the exponents of the power laws for v_{hs} , r_{hs} , L_{hs} , P_{hs} , n_{hs} are listed in Table 5.

Model IIa represents the self-similar evolution of sources with constant advance speed (what may be true, as indicated by the measurements of hot spot advance speeds, at least for the inner 100 parsecs). The decrease of density with linear size with an exponent of -2 is consistent with the values derived by other authors for larger scales (Fanti et al. 1995, Begelman 1996, De Young 1993, 1997). Comparing with Model I, we see that constraining γ to 1.0 leads to a decrease in luminosity while maintaining the hot spot expansion work. The values of the exponents for P_{hs} and n_{hs} are in agreement (within the respective error bars) with those obtained in the fits. The energy required for the source to grow and expand at constant rate in the present model without increasing the jet power supply (remember that now $\gamma = 1$) comes from a decrease in luminosity. In our model this decrease of the hot spot luminosity is produced by the fast reduction of pressure in the hot spot (caused by its fast expansion). However the required luminosity decrease ($\propto (LS)^{-0.5}$) is quite far from the value derived for the $L_{\text{hs}}-LS$ plot (despite its large error bar).

Model IIb represents an extreme opposite case of Model IIa. Now, besides self-similarity, we force the source to increase its luminosity at the rate prescribed by the fit ($\propto (LS)^{0.3}$). The crucial parameter is, again the density profile in the external medium that controls the expansion rate of the hot spot and the

pressure decrease. The small external density gradient makes the source to decelerate its expansion rate maintaining a large pressure. The values of the exponents of the hot spot pressure and density power laws are compatible (within the corresponding error bars) with those derived from the fits. The deceleration rate for the hot spot advance is large but plausible if one takes into account that the CSO hot spot advance speeds measured up to now (Owsianik & Conway 1998, Owsianik et al. 1998b, Taylor et al. 2000) are all for small sources (≤ 100 pc) which leaves lot of freedom for the hot spot advance speed profile in the first kpc. On the other hand the slowly decreasing external density profile ($\propto (LS)^{-1.1}$) is consistent with the structure of the ISM in ellipticals well fitted by King profiles with almost constant density galaxy cores 1 kpc wide. One model with constant external density ($\delta = 0$) and self-similar expansion would have resulted in an increase of luminosity with distance to the source proportional to $(LS)^{1.25}$ and a decrease in hot spot pressure and advance speed as $(LS)^{-1}$. Such a large increase in luminosity is hardly compatible with the fit presented in section (3). Moreover, a density gradient like the one obtained in Model IIb allows for a smooth transition between the density in the inner core (which could be constant) and the gradient in outer regions, likely -2 .

Finally let us note that our hypothesis allow for a continuous transition between Models IIa and IIb by tuning the value of the exponent of the density power law between 1.1 and 2.0. In particular, the model with $\delta = 1.6$ fits very well the exponents of hot spot pressure (and relativistic particle density) and predicts evolutive behaviours for L_{hs} and v_{hs} in reasonable agreement with the observable data ($L_{\text{hs}} \propto LS^{-0.14}$ and $v_{\text{hs}} \propto LS^{-0.2}$).

6. DISCUSSION

Results of the fits presented in section (3) show that sources evolve very close to self-similarity in the first kiloparsec of their lives. This result agrees with what has been found by other groups. Snellen et al. (2000) calculate equipartition component sizes for a sample of GPS and CSS sources (Snellen et al. 1998a, Stanghellini et al. 1998, and Fanti et al. 1990) finding a proportionality with projected source overall size. Jeyakumar & Saikia (2000) find self-similarity in a sample of GPS and CSS sources up to 20 kpc. Concerning the dependence of radio luminosity with linear size, the fit shown in section (3) points towards an increase of luminosity with linear size, as claimed by Snellen et al. (2000) for GPS sources. However, uncertainties are large and this dependence has to be confirmed by new CSO and GPS samples.

As established in the Introduction, our study on CSOs offers an interesting link between fundamental parameters of the jet production process and the properties of large scale jets. It is interesting to note, on one hand, that the lower bound for the jet power is consistent (one order of magnitude larger) with the one inferred by Rawlings & Saunders (1991) for FR II radio galaxies (10^{44} erg s^{-1}), supporting the idea of CSOs being the early phases of FR IIs. On the other hand, the flux of particles inferred in the jet is consistent with ejection rates of barionic plasma of the order $0.17 M_{\odot} y^{-1}$, implying a highly efficient conversion of accretion mass at the Eddington limit ($\dot{M}_{\text{E}} \simeq 2.2 M_{\odot} y^{-1}$, for a black hole of $10^8 M_{\odot}$) into ejection. The need for such a high efficiency could also point towards a leptonic composition of jets. Central densities can be estimated using the ram pressure equilibrium assumption for those sources with have measured advance speeds, from the follow-

ing equation equivalent to (8) $P_{\text{hs}} = \rho_{\text{ext}} v_{\text{hs}}^2$. Results range from $1 - 10 \text{ cm}^{-3}$ for 0108+108 which is close to the galactic nucleus, to $0.01 - 0.1 \text{ cm}^{-3}$ for 2352+495 which is about 100 pc away.

Our study concentrates in the evolution of sources within the first kpc assuming energy equipartition between particles and magnetic fields and hot spot advance in ram pressure equilibrium, extending the work of Readhead et al. (1996a,b) to a larger sample. In Readhead et al. (1996b) the authors construct an evolutionary model for CSOs based on the data of three sources (0108+388, 0710+439, 2352+495) also in our sample. Comparing the properties of the two opposite hot spots in each source these authors deduce a value for the advance speed as a power law of external density approximately constant which fixes the remaining dependencies: $P_{\text{hs}} \propto \rho_{\text{ext}}^{1.00}$, $r_{\text{hs}} \propto \rho_{\text{ext}}^{-0.50}$. These results fit very well with those obtained in our Model IIa. Model IIb could be understood as complementary to Model IIa and represent a first epoch in the early evolution of CSOs. It describes the evolution of a source in an external medium with a smooth density gradient, causing the decrease of the hot spot advance speed. During this first epoch, the luminosity of the source would increase. Then, the change in the external density gradient (from -1.1 to -2.0) will stop the deceleration of the hot spots and would change the sign of the slope of luminosity, which now would start to decrease (Model IIa).

To know whether CSOs evolve according to Model IIa or IIb (or a combination of both, IIb+IIa) needs fits of better quality. However, what seems clear is that models with constant hot spot advance speed and increasing luminosity (i.e., Model I) can be ruled out on the ground of their energy costs.

We can calculate the age of a source when it reaches 1 kpc (the edge of the inner dense galactic core) according to Models IIa and IIb assuming an initial speed (let say at 10 pc) of 0.2 c (as suggested by recent measurements). In the case of Model IIa this age is of $3.3 \cdot 10^4$ y, whereas in the case of Model IIb the age is about one order of magnitude larger (i.e., $\simeq 1.1 \cdot 10^5$ y). In this last case, the source would reach this size with a speed of 0.02 c. If hot spots advance speeds remain constant after 1 kpc (consistent with a density gradient of slope -2.0 , commonly obtained in fits for large scale sources; see below) then the age of a source of size 100 kpc would be of the order $1.6 \cdot 10^7$ y. This result supports CSOs as precursors of large FR II radio sources.

Since the work of Carvalho (1985) considering the idea of compact doubles being the origin of extended classical doubles, several attempts have been made to describe the evolution of CSOs to large FR II sources. Fanti et al. (1995) discussed a possible evolutionary scenario based on the distribution of sizes of a sample of CSS sources of *medium* size (< 15 kpc), assuming equipartition and hot spot advance driven by ram pressure equilibrium. Their model supports the young nature of MSOs predicting a decrease in radio luminosity by a factor of ten as they evolve into more extended sources and that external density changes as $(LS)^{-2}$ after the first half kiloparsec.

Begelman's (1996) model predicts an expansion velocity depending only weakly on source size and a evolution of luminosity proportional to $\approx (LS)^{-0.5}$ for ambient density gradients ranging from $(LS)^{-(1.5-2.0)}$. It accounts for the source statistics and assumes Begelman & Cioffi's (1989) model for the evolution of cocoons surrounding powerful extragalactic radio sources. This means constant jet power, hot spot advance driven by ram pressure equilibrium, internal hot spot conditions near equipartition, and that internal pressure in the hot-spots is equal

to that in the cocoon multiplied by a constant factor, condition which turns to be equivalent to self-similarity. Snellen et al. (2000) explain the GPS luminosity function with a self-similar model, assuming again constant jet power. The model predicts a change in the slope of the radio luminosity after the first kpc ($\propto (LS)^{2/3}$ in the inner region; decreasing at larger distances), governed by an external density King profile falling with $(LS)^{-1.5}$ outside the 1 kpc core.

Model IIa predicts an external density profile in agreement with those inferred in the long term evolution models just discussed. However, it leads to a decrease of the hot spot pressure ($\propto (LS)^{-2}$) too large. Readhead et al. (1996b) compare their data for CSOs with more extended sources (quasars from Bridle et al. 1994) and obtain a best fit for pressure $P_{\text{hs}} \propto (LS)^{-4/3}$, which is in agreement with our Model IIb. However, Model IIb produces a flat ($\propto (LS)^{-1.1}$) external density gradient and an unwelcome increase in radio luminosity. The conclusion is that neither Model IIa nor IIb can be directly applied to describe the complete evolution of powerful radio sources from their CSO phase. In Perucho & Martí (2001) we have plotted the same physical magnitudes than here versus projected linear size for sources that range from CSOs to FRIIs and the most remarkable fact is the almost constant slope found for pressure evolution. We try to reconcile the change of the slopes found for external density and luminosity with this behaviour of pressure by considering a time dependent (decreasing) jet power, in agreement with the jet powers derived for CSOs and FRIIs (a factor of 20 smaller the latter). In that paper, we have used the samples of MSOs given by Fanti et al. (1985) and FRIIs by Hardcastle et al. (1998) and estimated the relevant physical magnitudes in their hot spots as we have done for CSOs. The fit for the plot of hot-spot radius versus projected linear size shows the loss of self-similarity from 10 kpc on, a result which is consistent with that of Jeyakumar & Saikia (2000). Concerning radio luminosity, a clear break in the slope at 1 kpc is apparent, feature predicted by Snellen et al. (2000) for GPSs.

7. CONCLUSIONS

In this paper, we present a model to determine the physical parameters of jets and hot-spots of a sample of CSOs under very basic assumptions like synchrotron emission and minimum energy conditions. Based on this model we propose a simple evolutionary scenario for these sources assuming that they evolve in ram pressure equilibrium with the external medium and constant jet power. The parameters of our model are constrained from fits of observational data (radio luminosity, hot spot radius, and hot spot advance speeds) and hot spot pressure versus projected linear size. From these plots we conclude that CSOs evolve self-similarly (Jeyakumar & Saikia 2000) and that their radio luminosity increases with linear size (Snellen et al. 2000) along the first kiloparsec.

Assuming that the jets feeding CSOs are relativistic from both kinematical and thermodynamical points of view, hence neglecting the effects of any thermal component, we use the values of the pressure and particle number density within the hot spots to estimate the fluxes of momentum (thrust), energy, and particles of these relativistic jets. We further assume that hot spots advance at subrelativistic speeds and that there is ram pressure equilibrium between the jet and hot spot. The mean jet power obtained in this way is, within an order of magnitude, that given by Rawlings & Saunders (1991) for FRII sources, which is consistent with them being the possible precursors of

large doubles. The inferred flux of particles corresponds to, for a barionic jet, about a 10% of the mass accreted by a black hole of $10^8 M_{\odot}$ at the Eddington limit, pointing towards a very efficient conversion of accretion flow into ejection, or to a leptonic composition of jets.

We have considered three different models (namely Models I, IIa, IIb). Model I assuming constant hot spot advance speed and increasing luminosity can be ruled out on the ground of its energy cost. However Models IIa and IIb seem to describe limiting behaviours of sources evolving at constant advance speed and decreasing luminosity (Model IIa) and decreasing hot spot advance speed and increasing luminosity (Model IIb). However, in order to know whether CSOs evolve according to Model IIa or IIb (or a combination of both, IIb+IIa) we need fits of better quality and more determinations of the hot spot advance speeds and radio-luminosity. In all our models the slopes of the hot spot luminosity and advance speed with source linear size are governed by only one parameter, namely the external density gradient.

Terminal speeds obtained for Model IIb, in which we find a negative slope for the hot spot advance speed, are consistent with advance speeds inferred for large sources like Cygnus A (Readhead et al. 1996b). This fact, together with the ages estimated from that model and the recent measures of advance speed of CSOs (Owsianik et al. 1998, Taylor et al. 2000) support the young scenario for CSOs. Moreover, central densities estimated in section (6) using ram pressure equilibrium assumption are low enough to allow jets with the calculated kinetic powers to escape (De Young 1993). External density profile in Model IIa is consistent with that given for large sources (-2.0), while Model IIb gives a smoother profile as corresponds to a King profile in the inner kiloparsec.

Although Models II seem to describe in a very elegant way the evolution of CSOs within the first kpc, preliminary results show that neither Model IIa nor IIb can be directly applied to describe the complete evolution of powerful radio sources from their CSO phase. In Perucho & Martí (2001) we try to reconcile the change of the slopes of external density and luminosity with the behaviour of pressure (see discussion section) by considering a time dependent (decreasing) jet power.

We thank A. Peck and G.B. Taylor for the data they provided us. We thank D.J. Saikia for his interest in our work and supply of information about his papers, which were very useful for us. This research was supported by Spanish Dirección General de Investigación Científica y Técnica (grants DGES-1432).

APPENDIX: OBTAINING BASIC PHYSICAL PARAMETERS FROM OBSERVATIONAL DATA

1. INTRINSIC LUMINOSITIES AND SIZES

We obtain the required parameters by using observational data in a simple way. The first step is to obtain the luminosity distance to the source, in terms of redshift and the assumed cosmological model,

$$D_L = \frac{cz}{H_0} \left(\frac{1 + \sqrt{1 + 2q_0z + z}}{1 + \sqrt{1 + 2q_0z + q_0z}} \right) \quad (27)$$

Angular distance, used to obtain intrinsic linear distances, is defined as

$$D_{\theta} = \frac{D_L}{(1+z)^2} \quad (28)$$

Intrinsic linear distances (like the source linear size, LS , and hot spot radius, r_{hs}) are obtained from the source angular distance and the corresponding angular size of the object

$$LS = D_{\theta} \theta_T / 2, \quad r_{\text{hs}} = D_{\theta} \theta_{\text{hs}} \quad (29)$$

with θ_T being the total source angular size, and θ_{hs} the angular size of the hot spot, given in Table 1. The intrinsic total radio luminosity of the hot spots can be obtained in terms of the observed flux density, S_{hs} , and the luminosity distance according to

$$L_{\text{hs}} = 4\pi D_L^2 S_{\text{hs}}, \quad (30)$$

where S_{hs} corresponds to the total flux in the frequency range $10^7 - 10^{11}$ Hz (ν_{min} , ν_{max} , in the following)

$$S_{\text{hs}} = \int_{\nu_{\text{min}}}^{\nu_{\text{max}}} C(\nu)^{-\alpha} d\nu. \quad (31)$$

The constant for the spectrum in the observer reference frame can be obtained from the flux density at a given frequency (ν_0) and the spectral index, having in mind that the synchrotron spectra in the optically thin limit follows a power law

$$C = S_{\nu_0} (\nu_0)^{\alpha}. \quad (32)$$

Hence, in terms of known variables, the total intrinsic radio luminosity is written as follows

$$L_{\text{hs}} = S_{\nu_0} 4\pi D_L^2 \nu_0^{\alpha} \frac{(\nu_{\text{max}})^{1-\alpha} - (\nu_{\text{min}})^{1-\alpha}}{1-\alpha} \quad (\alpha \neq 1) \quad (33)$$

$$L_{\text{hs}} = S_{\nu_0} 4\pi D_L^2 \nu_0^{\alpha} \ln \left(\frac{\nu_{\text{max}}}{\nu_{\text{min}}} \right) \quad (\alpha = 1). \quad (34)$$

2. MINIMUM ENERGY ASSUMPTION

Once obtained intrinsic sizes and luminosities from observations, the next step is to use them to constrain physical parameters (like pressure, magnetic field strength, and relativistic particle density) in the hot spots. Our model is based on the minimum energy assumption according to which the magnetic field has such a value that total energy of the object is the minimum necessary so as to produce the observed luminosity. As it is well known, this assumption leads almost to the equipartition of energy between particles and magnetic field.

The total internal energy of the system can be written in terms of the magnetic field strength, B . First, the energy density of the relativistic particles

$$u_p = \int_{E_{\text{min}}}^{E_{\text{max}}} n(E) E dE \quad (35)$$

(where E is the energy of particles and $n(E)$, the number density at the corresponding energy) can be estimated assuming

monochromatic emission. According to this, any electron (of energy E) radiates only at its critical frequency, given by

$$\nu_c = C_1 B E^2, \quad (36)$$

where C_1 is a constant ($\simeq 6.3 \cdot 10^{18}$ in cgs units). The monochromatic emission assumption allows to change the energy integral in Eq.(35) by an integral of the intrinsic emitted flux in the corresponding range of critical frequencies. At the end, the total internal particle energy in the hot spots, U_p , is (see, e.g., Moffet 1975)

$$U_e = A L_{\text{hs}} B^{-3/2}, \quad (37)$$

where A depends on the spectral index and the frequency range:

$$A = \frac{C_1^{1/2}}{C_3} \frac{2 - 2\alpha}{1 - 2\alpha} \frac{\nu_{\text{max}}^{(1/2)-\alpha} - \nu_{\text{min}}^{(1/2)-\alpha}}{\nu_{\text{max}}^{1-\alpha} - \nu_{\text{min}}^{1-\alpha}}, \quad (38)$$

($C_3 \simeq 2.4 \cdot 10^{-3}$ in cgs units). Limits for the radio-emission frequencies are taken to be 10^7 and 10^{11} Hz. A varies within a factor of six ($3.34 \cdot 10^7$, $2.2 \cdot 10^8$) for extreme values of the spectral index, α (0.75, 1.5, respectively).

Then, the expression for the total internal energy in the hot spot is

$$U_{\text{tot}} = U_p + U_B = A L_{\text{hs}} B^{-3/2} + V_{\text{hs}} \frac{B^2}{8\pi}, \quad (39)$$

where V_{hs} is the volume of the hot spot (assumed spherical) and $B^2/8\pi$ is the magnetic field energy density. The magnetic field which gives the minimum energy for the component comes directly from minimising equation (39), leaving as constant the intrinsic luminosity of the hot spot, L_{hs} ,

$$B_{\text{min}} = \left(\frac{6\pi A L_{\text{hs}}}{V_{\text{hs}}} \right)^{2/7}, \quad (40)$$

Hence, the energies associated to magnetic field and relativistic particles are, finally,

$$u_B = \frac{B_{\text{min}}^2}{8\pi}, \quad (41)$$

and

$$u_p = (4/3)u_B. \quad (42)$$

Pressure at the hot spots has two contributions

$$P_{\text{hs}} = (1/3)u_p + (1/3)u_B = (7/9)u_B. \quad (43)$$

The number density of relativistic particles follows from the monochromatic emission assumption:

$$n_{\text{hs}} = \frac{L_{\text{hs}} C_1}{C_3 B_{\text{min}} V_{\text{hs}}} \frac{2\alpha - 2}{2\alpha} \frac{\nu_{\text{max}}^{-\alpha} - \nu_{\text{min}}^{-\alpha}}{\nu_{\text{max}}^{1-\alpha} - \nu_{\text{min}}^{1-\alpha}}. \quad (44)$$

REFERENCES

- Begelman, M.C. 1996, in proc. of the Greenbank Workshop, Cygnus A-study of a Radio Galaxy, ed. Carilli, C.L., Harris D.E. (CUP, Cambridge), 209
 Bicknell, G.V., Dopita, M.A., O'Dea, C.P. 1997, ApJ, 485, 112
 Bondi, M., Garrett, M.A. & Gurvits, L.I. 1998, MNRAS 297, 559
 van Breugel, W.J.M., Miley, G.K., Heckman, T.A. 1984, AJ, 89, 5
 Carvalho, J.C. 1985, MNRAS, 215, 463
 Carvalho, J.C. 1994, A&A, 292, 392
 Carvalho, J.C. 1998, A&A, 329, 845
 Conway, J.E., Pearson, T.J., Readhead, A.C.S., Unwin, S.C., Xu, W., & Mutel, R.L. 1992, ApJ, 396, 62
 Conway, J.E., Myers, S.T., Readhead, A.C.S., Unwin, S.C., & Xu, W. 1994, ApJ, 425, 568
 Dallacasa, D., Fanti, C., Fanti, R., Schilizzi, R.T., & Spencer, R.E. 1995, A&A, 295, 27

- Dallacasa, D., Bondi, M., Alef, W., & Mantovani, F. 1998, *A&AS* 129, 219
- De Young, D.S. 1991, *ApJ*, 371, 69
- De Young, D.S. 1993, *ApJ*, 402, 95
- De Young, D.S. 1997, *ApJL*, 490, 55
- Fanti, C., Fanti, R., Parma, P., Schilizzi, R.T., & van Breugel, W.J.M. 1985, *A&A*, 143, 292
- Fanti, R., Fanti, C., Spencer, R.E., Nan Rendong, Parma, P., van Breugel, W.J.M., & Venturi, T. 1990, *A&A*, 231, 333
- Fanti, C., Fanti, R., Dallacasa, D., Schilizzi, R.T., Spencer, R.E., & Stanghellini, C. 1995, *A&A*, 302, 317
- Fey, A.L., Clegg, A.W., & Fomalont, E.B. 1996, *ApJS*, 105, 299
- Güijosa, A., Daly, R.A. 1996, *ApJ*, 461, 600
- Hardcastle, M.J., Alexander, P., Pooley, G.G., & Riley, J.M. 1998, *MNRAS*, 296, 445
- Jeyakumar, S., & Saikia, D.J. 2000, *MNRAS*, 311, 397
- Jeyakumar, S., Saikia, D.J., Pramesh Rao, A., Balasubramanian 2000, *astro-ph/0008288*
- Kuncic, Z., Bicknell, G.V., & Dopita, M.A. 1998, *ApJL*, 495, 35
- Martí, J.M², Müller, E., Font, J.A., Ibáñez, J.M², & Marquina, A. 1997, *ApJ*, 479, 151
- Moffet, A. 1975, in vol. IX, *Galaxies and the Universe, Stars and Stellar Systems*, ed. Sandage, A.R. (University of Chicago Press)
- Mutel, R.L., Hodges, M.W., & Phillips, R.B. 1985, *ApJ*, 290, 86
- Mutel, R.L., & Hodges, M.W. 1986, *ApJ*, 307, 472
- Mutel, R.L., & Phillips, R.B. 1988, *IAUS*, 129, 73
- O'Dea, C.P., Baum, S.A., & Stanghellini, C. 1991, *ApJ*, 380, 66
- O'Dea, C.P., & Baum, S.A. 1997, *AJ*, 113, 148
- O'Dea, C.P. 1998, *PASP*, 110, 493
- Owsianik, I., & Conway, J.E. 1998, *A&A*, 337, 69
- Owsianik, I., Conway, J.E., & Polatidis, A.G. 1998, *A&AL*, 336, 37
- Owsianik, I., Conway, J.E., & Polatidis, A.G. 1999, *NewAR*, 43, 669
- Pearson, T.J., & Readhead, A.C.S. 1988, *ApJ*, 328, 114
- Peck, A.B., & Taylor, G.B. 2000, *ApJ*, 534, 90
- Peck, A.B., & Taylor, G.B. 2000, *ApJ*, 534, 104
- Peck, A.B. 2000, private communication
- Perucho, M., & Martí, J.M², in preparation
- Phillips, R.B., & Mutel, R.L. 1980, *ApJ*, 236, 89
- Phillips, R.B., & Mutel, R.L. 1981, *ApJ*, 244, 19
- Phillips, R.B., & Mutel, R.L. 1982, *A&A*, 106, 21
- Readhead, A.C.S., Taylor, G.B., Xu, W., Pearson, T.J., Wilkinson, P.N., & Polatidis, A.G. 1996a, *ApJ*, 460, 612
- Readhead, A.C.S., Taylor, G.B., Pearson, T.J., & Wilkinson, P.N. 1996b, 460, 634
- Snellen, I.A.G., Schilizzi, R.T., de Bruyn, A.G., Miley, G.K., Rengelink, R.B., Rötgering, H.J.A., Bremer, M.N. 1998a, *A&AS*, 131, 435
- Snellen, I.A.G., Schilizzi, R.T., de Bruyn, A.G., & Miley, G.K. 1998, *A&A*, 333, 70
- Snellen, I.A.G., Schilizzi, R.T., Miley, G.K., de Bruyn, A.G., Bremer, M.N., Rötgering, H.J.A. 2000, *astro-ph/0002130*
- Snellen, I.A.G., Schilizzi, R.T., Miley, G.K., Bremer, M.N., Rötgering, H.J.A., & van Langevelde, H.J. 1999, *NewAR*, 43, 675
- Snellen, I.A.G., & Schilizzi, R.T. 1999, in "Perspectives on Radio Astronomy: Scientific Imperatives at cm and mm Wavelengths" (Dwingeloo: NFRA), ed. M.P. van Haarlem & J.M. van der Hulst, *astro-ph/9907170*
- Snellen, I.A.G., & Schilizzi, R.T. 1999, invited talk at 'Lifecycles of Radio Galaxies' workshop, ed. J. Biretta et al. (*New Astronomy Reviews*), *astro-ph/9911063*
- Snellen, I.A.G., Schilizzi, R.T., & van Langevelde, H.J. 2000, *astro-ph/0002129*
- Stanghellini, C., O'Dea, C.P., Baum, S.A., Dallacasa, D., Fanti, R., Fanti, C. 1997, *A&A*, 325, 943
- Stanghellini, C., O'Dea, C.P., Dallacasa, D., Baum, S.A., Fanti, R., Fanti, C. 1998, *A&AS*, 131, 303
- Stanghellini, C., O'Dea, C.P., & Murphy, D.W. 1999, *A&AS*, 134, 309
- Taylor, G.B., Readhead, A.C.S., & Pearson, T.J. 1996, *ApJ*, 463, 95
- Taylor, G.B., & Vermeulen, R.C. 1997, *ApJL*, 485, 9
- Taylor, G.B., Marr, J.M., Pearson, T.J., & Readhead, A.C.S. 2000, accepted to the *ApJ*, *astro-ph/0005209*
- Wilkinson, P.N., Polatidis, A.G., Readhead, A.C.S., Xu, W., & Pearson, T.J. 1994, *ApJL*, 432, 87
- Xu, W., Readhead, A.C.S., Pearson, T.J., Polatidis, A.G., & Wilkinson, P.N. 1995, *ApJS*, 99, 297

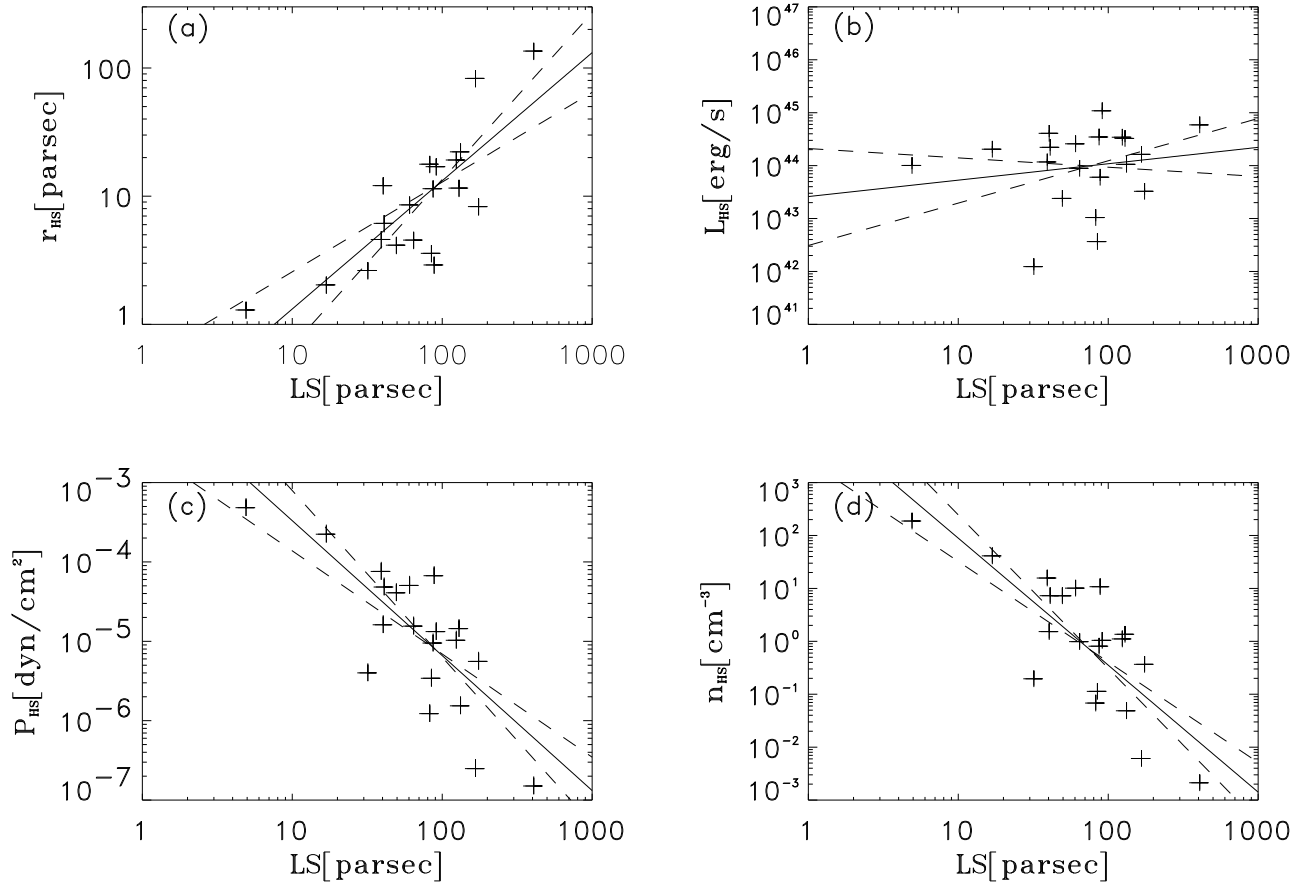


FIG. 1.— Log-log plots of radius (panel a), radio-luminosity (panel b), pressure (panel c) and density (panel d) of hot-spots versus projected linear size. One point per CSO is plotted (see text). Error bars correspond to 15% in angular sizes for radius, pressure and density and 15% in measured radio-flux at the given frequency for radio-luminosity, and they are just indicative. Dashed lines give account of limiting slopes.

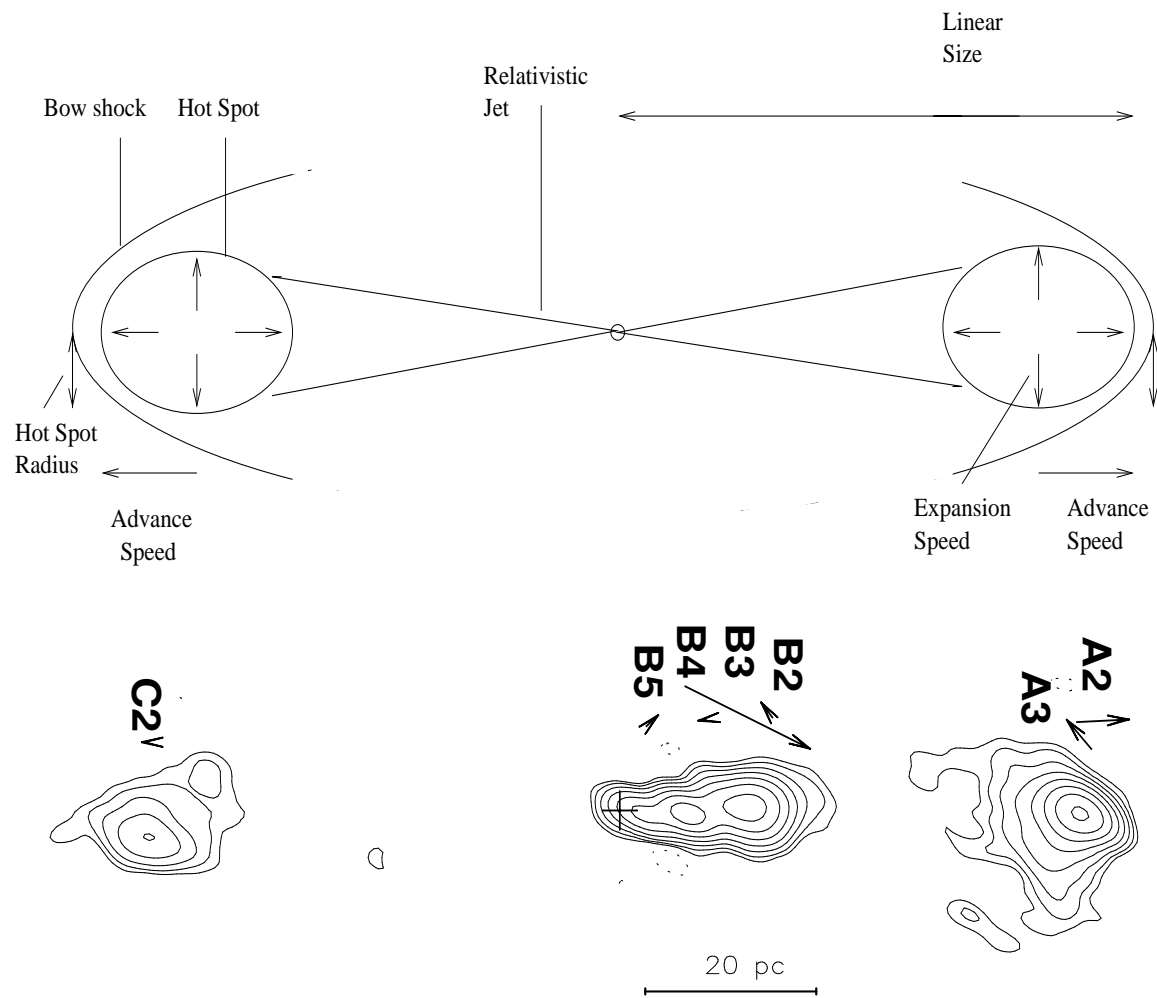


TABLE 1

Source	θ (mas)	θ_T (as)	Spectral index(α)	z	ν (GHz)	S_ν (Jy)	Refs.
0108+388S	0.821	0.006	0.900	0.669	15.36	0.118	1,2,3
0108+388N	0.586	0.006	0.900	0.669	15.36	0.172	1,2,3
0404+768E	45.0	0.150	0.501	0.599	1.70	0.429	1,2,7
0404+768W	54.0	0.150	0.501	0.599	1.70	4.181	1,2,7
0500+019N	5.17	0.015	0.900	0.583	8.30	1.25	1,5,10
0500+019S	3.49	0.015	0.900	0.583	8.30	0.110	1,5,10
0710+439N	0.950	0.025	0.600	0.518	8.55	0.330	1,3,4
0710+439S	2.16	0.025	0.600	0.518	8.55	0.110	1,3,4
0941-080N	7.637	0.050	1.01	0.228	8.30	0.080	1,5
0941-080S	12.7	0.050	1.01	0.228	8.30	0.130	1,5
1031+5670W	1.047	0.036	1.10	0.460	15.3	0.080	17
1031+5670E	1.296	0.036	0.80	0.460	15.3	0.065	17
1111+1955N	2.800	0.020	1.50	0.299	8.40	0.126	17,18,19,20
	1.070						
1111+1955S	1.370	0.020	1.50	0.299	8.40	0.090	17,18,19,20
1117+146N	4.40	0.080	0.800	0.362	22.9	0.050	1,11
1117+146S	2.90	0.080	0.800	0.362	22.9	0.100	1,11
1323+321N	9.83	0.060	0.600	0.369	8.55	0.700	1,4
1323+321S	10.28	0.060	0.600	0.369	8.55	0.380	1,4
1358+624N	27.0	0.070	0.700	0.431	1.663	1.152	1,4
1358+624S	40.2	0.070	0.700	0.431	1.663	2.601	1,4
1404+286N	0.990	0.007	1.60	0.077	8.55	1.67	1,4
	1.19						
1404+286S	2.14	0.007	1.60	0.077	8.55	0.140	1,4
	0.380						
1414+455N	3.20	0.034	1.62	0.190	8.40	0.042	17,18,19,20
1414+455S	2.30	0.034	1.52	0.190	8.40	0.034	17,18,19,20
	1.15						
1607+268N	3.78	0.050	1.20	0.473	5.00	0.840	1,13
	6.66						
1607+268S	6.48	0.050	1.20	0.473	5.00	0.740	1,13
	6.66						
1732+094N	1.947	0.015	1.10	0.610	5.00	0.480	1,15
1732+094S	2.48	0.015	1.10	0.610	5.00	0.285	1,15
1816+3457N	4.46	0.035	1.92	0.245	8.40	0.028	17,18,19,20
1816+3457S	4.57	0.035	1.85	0.245	8.40	0.074	17,18,19,20
	1.67						
	3.73						
1946+704N	1.46	0.036	0.640	0.101	14.9	0.122	8,9
	2.42						
1946+704S	3.27	0.036	0.640	0.101	5.00	0.019	8,9
2008-068N	2.74	0.030	0.800	0.750	5.00	1.01	1,15
2008-068S	4.68	0.030	0.800	0.750	5.00	0.112	1,15
2050+364W	3.06	0.060	0.900	0.354	5.00	2.11	1,12,13,14
2050+364E	5.22	0.060	0.900	0.354	5.00	2.89	1,12,13,14
	3.60						
	4.50						
2128+048N	4.62	0.030	0.800	0.990	8.30	1.21	1,5,10
	5.80						
2128+048S	3.82	0.030	0.800	0.990	8.30	0.060	1,5,10
2352+495N	1.10	0.050	0.501	0.237	5.00	0.080	1,2,16
2352+495S	2.60	0.050	0.501	0.237	5.00	0.040	1,2,16

NOTE.— Data in the columns: (1) B1950.0 coordinates (N means northern hot-spot, S southern, etc.); (2) angular size (θ) of the hot spots (or subcomponents); (3) total angular size of the radio source, (θ_T); (4) spectral index, α , of the optically thin part of the spectrum; (5) source redshifts, z; (6) and (7) frequency (ν) and flux density (S_ν) at that frequency of the optically thin part of the spectrum for the whole hot spot (adding the fluxes of subcomponents if necessary); (8) references from which the data of each source have been taken. In those cases in which no spectral index for each hot spot were available, we have used that of the whole source. Angular sizes were taken for the highest frequency available in order to eliminate the contribution of the diffuse component. The angular sizes of components have been calculated by multiplying the geometric mean of the FWHM Gaussian axes by a factor 1.8, following Readhead et al. (1996a), in order to have spherical hot spots.

REFERENCES.— (1) Stanghellini et al. 1998, A&AS, 131, 303; (2) Taylor et al. 1996, ApJ, 463, 95; (3) Pearson et al. 1988, ApJ, 328, 114; (4) Fey et al. 1996, A&AS, 105, 299; (5) Dallacasa et al. 1998, A&AS, 129, 219; (6) Xu et al. 1995, A&AS, 99, 297; (7) Dallacasa et al. 1995, A&AS, 295, 27; (8) Snellen et al. 1998a, A&AS, 131, 435; (9) Snellen et al., astro-ph/0002129; (10) Stanghellini et al. 1997, A&A, 325, 943; (11) Bondi et al. 1998, MNRAS, 297, 559; (12) Phillips & Mutel 1981, ApJ, 244, 19; (13) Mutel et al. 1985, ApJ, 290, 86; (14) Mutel et al. 1986, ApJ, 307, 472; (15) Stanghellini et al. 1999, A&AS, 134, 309; (16) Readhead et al. 1996a, ApJ, 460, 612; (17) Taylor et al., astro-ph/0005209; (18) Peck & Taylor 2000, ApJ, 534, 104; (19) Peck et al. 2000, ApJ, 534, 90; (20) A. Peck 2000, private communication. (c):detected core.

TABLE 2
BEST FITS OF PHYSICAL PARAMETERS IN HOT-SPOTS IN TERMS OF SOURCE LINEAR SIZE.

	α	ε	r
r_{hs}	1.0	0.3	0.80
L_{hs}	0.3	0.5	0.17
P_{hs}	-1.7	0.4	-0.79
n_{hs}	-2.4	0.5	-0.78

NOTE.— α is the slope of the corresponding log-log best fit, ε is the error of that fit, and r is the regression coefficient.

TABLE 3
HOT-SPOT ADVANCE SPEED VALUES

Source	Owsianik et al.	Taylor et al.	LS (pc)
0108+388	$0.098 h^{-1} c$	$0.12 h^{-1} c$	17
0710+439	$0.13 h^{-1} c$	$0.26 h^{-1} c$	64
1031+567	-	$0.31 h^{-1} c^{\text{a}}$	88
2352+495	$0.13 h^{-1} c^{\text{b}}$	$0.16 h^{-1} c$	85

^a Speed measured for one hot spot and, possibly, a jet component.

^b Calculated from synchrotron ageing data from Readhead et al. (1996a).

TABLE 4
POWERS INVESTED BY THE JETS IN THEIR EVOLUTION.

	L_{hs}	$\dot{U}_{\text{int,hs}}$	Q_{adv}	$Q_{\text{exp,hs}}$
Power	$(2.2 \pm 2.1) 10^{44}$	$(8.3 \pm 7.8) 10^{43}$	$(2.5 \pm 1.9) 10^{44}$	$(1.9 \pm 1.8) 10^{44}$
Fraction	0.16 ± 0.16	0.06 ± 0.06	0.19	0.14 ± 0.14

NOTE.— Values are in erg s^{-1} . Fractions are over $Q_{\text{j,min}}$. Errors are calculated as for jet parameters.

TABLE 5
EXPONENTS OF EVOLUTION FOR MODELS IIA AND IIB

Model	β	δ	r_{hs}	L_{hs}	v_{hs}	P_{hs}	n_{hs}
Ia	1.0 ± 0.3	2.0 ± 0.6	1.0	-0.50 ± 0.15	0.0	-2.0 ± 0.6	-2.50 ± 0.75
Ib	0.7 ± 0.3	1.1 ± 1.0	1.0	0.3	-0.5 ± 0.4	-1.5 ± 0.8	-1.9 ± 1.0

NOTE.— Exponents of the linear size power law fits of the physical parameters in the CSO hot spots for Models Ia and Ib. Errors, as before, were obtained from the extreme values given by the errors obtained for the slopes in the fits.